HIGH-T_C SUPERCONDUCTIVITY IN IRON-BASED PNICTIDES AND CHALCOGENIDES

Shailaj Kumar Shrivastava[1] and Girijesh Kumar[2]
[1]Principal, A.M. College, Gaya, Bihar, India
[2]Professor (Assistant), M.S.Y. College, Jahanabad, Bihar, India

Abstract: Iron based superconductors have a high superconducting transition temperature (T_c), a large critical current density (J_c), a very high upper critical field (H_{c2}) and a low anisotropy (γ). Electronic properties of the iron based superconductor are critical for understanding its phase diagram, mechanism and transport properties. In this paper we describe the progress of research on material classification, electronic structure, phase diagram, superconducting properties and applications of iron based superconductors.

Index Terms: Transition temperature, electron correlation, pairing, phase diagram, Bad metal.

I. INTRODUCTION

The discovery of superconductivity in an iron pnictides and chalcogenides raised the prospect of finding high-T_c superconductivity in compounds other than copper-based materials. The highest T_c of all iron based superconductors was found in the 1111- compound (T_c~58K) [1], which places this compound between the cuprates and MgB_2. In iron based superconductors, superconductivity pairing does not arise from the conventional electron-phonon coupling because electron-phonon coupling is believed to be incapable of introducing such a high temperature in these compounds. It may be due to consequence of an unconventional pairing mechanism generated by electron-electron Coulomb interaction. Two important characteristics of iron based superconductors provide an indication of the mechanism behind their unconventional superconductivity: first, in the phase diagram, superconductivity emerges out of a 'bad metal' normal state; second, the superconducting phase occurs near the onset of antiferromagnetic (AFM) order. The iron based superconductors share a common layered structure based upon a planar layer of iron atoms joined by tetrahedrally coordinated pnictogen(P,As) or chalcogen anions arranged in a stack sequence separated by alkali, alkaline earth or rare earth and oxygen/ fluorine 'blocking layers'. Pressure has an essential role in the production and control of superconductivity in iron based superconductors Substitution of a large cation by a smaller rare earth ion to stimulate the pressure effect has raised the superconducting transition temperature T_c to a record high of 55K in these materials [2]. It is general trend that the optimal T_c is higher in the order 1111> 122>11. Critical current J_c values exceeding 10^5 Acm^{-2} were measured in iron superconducting films of 11,122 and 1111 families up to very large magnetic field either parallel or perpendicular to the Fe planes. In this paper we present brief review of electronic, magnetic and superconducting properties of iron-pnictides and iron-chalcogenide superconductors.

II. MATERIALS AND ELECTRONIC STRUCTURE

Iron based superconductors including iron pnictides and iron chalcogenides are quasi two dimensional materials. They have very complicated electronic structures and competing interactions. Iron based superconductor was first discovered in LaFePO [3] with T_c ~4 K. Subsequently superconductivity was found in LaNiAsO [4] with T_c = 2.4 K and LaNiPO with T_c =3K. The critical temperature T_c jumped to 26 K for $LaFeAsO_{1-x}F_x$ (x=0.08) by replacing phosphorus with arsenic and some of the O atoms replaced by F atoms [5]. These materials contain a common building block of a square lattice of Fe^{2+} ions with tetrahedral coordination with Pn (P and/or As) or Ch ions. The T_c values of LaFeAs (O, F) raised to 43K by application of pressure [6]. An increased T_c up of 56 K was reported in $SmO_{1-x}F_xFeAs$ [7], $Gd_{1-x}Th_xFeAsO$ [8], $Sr_{1-x}Sm_xFeAsF$ [9] and $Ca_{1-x}Nd_xFeAsF$[10]. Iron based superconductors have been extended to a large variety of materials including four prototypical families of iron based superconductors 1111,122,111, and 11 types.

Further variations such as 42622 type iron Pnictides has an alternating layers stacking structure of antifluorite Fe_2P_2 and perovskite based $Sr_4Sc_2O_6$ oxide layers[11]. The space group of the material is P4/nmm, and the lattice constant a and c are 4.016 and 15.543Å respectively. Figure 1 shows the crystal structures for several types of iron based superconductors. The electronic structure of the iron based superconductors and related materials are characterized by the multiband and multiorbital nature [12]. All have 3d orbitals of Fe hybridize strongly with As and Se 4p orbitals They also couple strongly with each other and have contribution to both itinerant conducting electrons and localized magnetic moments. Based on their Fermi surface topology, one could divide them into two categories: a. Systems with both electrons and hole Fermi surfaces and b. System with only electron Fermi surface. The low energy electronic structure of iron based superconductors is dominated by the Fe 3d states [13]. The Fermi surface is usually composed of three-hole-like Fermi surfaces near the zone centre and two electron Fermi surfaces around the zone corner. The Fermi surface topology and band structure are rather similar for the 11,111,122 and 1111 series of iron based superconductors. The electronic structure of the iron-chalcogenide superconductor, $Fe_{1.04}(Te_{0.66}Se_{0.34})$ have clearly separated three bands with distinct even or odd symmetry that cross the Fermi energy (E_F) near the zone centre, which contribute to three hole like Fermi surfaces [14].

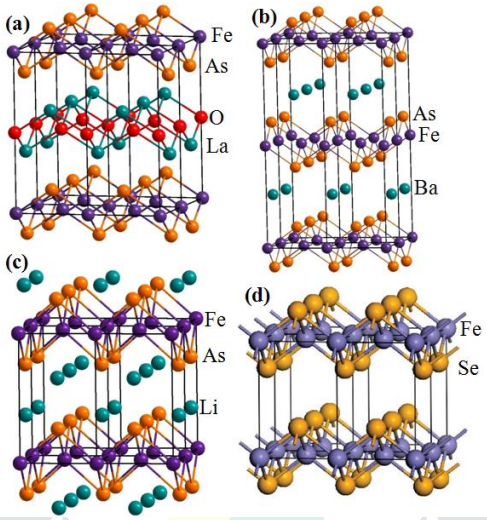

Figure1. Four families of iron-based superconductors,(a) 1111, (b) 122, (c) 111, (d) 11 type.

1111 family

The highest T_c~55K in iron based superconductor has been achieved in fluorine-doped or oxygen-deficient LnFeAsO compounds (Ln represents rare-earth metal atoms). LnFeAsO compounds have a tetragonal layered structure at room temperature with space group P4/nmm and lattice constants a=4.03268 Å, c=8.74111Å. For LaFeAsO(1111) compounds, which is a SDW or AFM metal where the electron appears to be more delocalized, the structure consists of alternate stacking of FeAs trilayer that are separated by fluoride- type LnO layers and the distance between the adjacent FeAs and LaO layers is 1.8 Å. With doping of F replacing O in part, $LaFeAsO_{0.89}F_{0.11}$ becomes superconducting. When small pressure is applied to $LaFeAsO_{0.89}F_{0.11,}$ T_c increases, reaching maximum value of T_c =43K at 4 GPa and then it decreases to T_c=9K at 30GPa [15].When the O^{2-} site is replaced with an F^- ion, the generated electron is transferred to the FeAs layer because of the energy offset between the layers.

The lattice constant a and c decreases with reducing the ion radii of the rare earth metal ions the optimal T_c first increases rapidly, reaching the highest T_c (55K) in the doped SmFeAsO system with fluorine doping [7] and then decreasing slightly with further reduction in radii of rare earth metal ions. The values of T_c (K) in 1111-type materials are shown in table 1.The atomic structure of the LaFePO consists of negatively charged FeP or FeAs layers, where Fe atoms form a planar square lattice, and positively charged LnO layers. With or without doping, electrons are conducting in FeP or FeAs layers. The electrical resistivity of pure LaFePO drops at 4K and that of F-doped LaFePO drops at higher temperature (~10K). The electronic structure of Fermi surface of LaFePO consists of five sheets, resulting from five bands which cross the Fermi level. Four of the five sheets are cylinder like along the K_z direction reflecting quasi two dimensional nature of atomic

structure , two of them are of hole type along the r-z high symmetry line of the Brillouin zone and other two are of electron type along the M-A line. The 5th sheet is a distorted hole type sphere centered at Z-high symmetry point. Electron doping into RE-1111 compounds (where RE = rare earth metal) was very successful, i.e., the max. T_c was increased from 26 K to 55 K by replacing La with other RE ion with smaller ionic radius. Recently a new 1111-type FeSe derived superconductor, $LiFeO_2Fe_2Se_2$ and T_c =43K was synthesized by Lu et al [16]. $LaFeAsO_{1-x}F_x$ superconducting materials contain a common building block of square lattice of Fe^{2+} ions which take tetrahedral coordination with P and/or As or chalcogenide ions. Since the Fermi level of each parent compound is primarily governed by Fe five 3d-orbitals, iron plays the central role of superconductivity. These compounds have tetragonal symmetry in the superconducting phase, are the Pauli paramagnetic metals in the normal state and undergo crystallographic/magnetic transition to orthorhombic or monoclinic anti-ferromagnetism at low temperatures. It was found that near the optimal doping of some iron pnictides, certain electron and hole pockets are better nested, they can overlap on each other when shifted [19] away from the optimal doping, the nesting worsen, since electron and hole pockets changes differently. Superconductivity was initially observed in iron pnictides with nested hole and electron Fermi pockets. However, for iron based superconductors there are both nodal and nodeless members [20]. The typical Fermi surfaces of iron pnictides comprises hole Fermi pockets in the middle of the Brillouin zone and electron Fermi pockets at the boundaries [21]. By contrast Li(Fe,Co)As which has almost perfectly nested Fermi packets is non-superconducting [22]. The geometry of the Fermi surface plays only a secondary role in superconductivity.

Table 1 T_c in 1111 type iron based superconductors along with the doping modes and pressure dependence.

System	Parent compound	T_c (K)	p (GPa)	
1111	CaFeAsF	29	5	
	CaFeAsH	28	3.3	
	$Ca(Fe_{1-x}Co_x)AsF$	24.7	1	
	SrFeAsF	25	16.5	
	$LaFeAsO_{0.89}F_{0.11}$	43	3	
	LaFeAsO	21	12	
	LaFePO	4	-	[3]
	$LaFeAsO_{0.65}H_{0.35}$	46	3	
	$LaFeAsO_{0.89}F_{0.11}$	9	30	
	$LaFeAsO_{0.89}F_{0.11}$	26	-	[5]
	SmFeAsO	11	9	
	$SmFeAsO_{0.9}F_{0.1}$	55	-	[7]
	$SmFeAsO_{0.85}$	41	7	
	$CeFeAsO_{0.84}F_{0.16}$	41	-	[17]
	$CeFeAsO_{0.88}F_{0.12}$	1.1	26.5	
	$NdFeAsO_{0.85}$	35	7	
	$NdFeAsO_{1-y}$	54.3	-	
	$PrFeAsO_{0.89}F_{0.11}$	52	-	[18]
	$GdFeAsO_{1-y}$	54	-	
	$Gd_{1-x}Th_xFeAsO$	56	-	
	$SmFeAsO_{1-x}F_x$	58.1		

The 122- type families

The 122 has the composition MFe_2As_2, where M is an alkaline earth element. To make them superconducting, the 122 compounds are usually doped with holes by replacing alkaline earths with alkali element. $BaFe_2As_2$ is a member of the 122 iron-pnictides family [23]; each unit cell contains two FeAs

trilayer separated by a layer of barium ions. In this class of materials, superconductivity arises following chemical substitution into the undoped compound as in the case of Ni_x substitution into $BaFe_2As_2$.In FeAs-122, the highest T_c~49K can be achieved in Pr-doped $CaFe_2As_2$ [24]. Superconductivity emerges when anti-ferromagnetism disappears or diminishes by carrier doping or structural modification by applying external pressure or by chemical pressure induced by isovalent substitution. However, the anti-ferromagnetism and superconductivity co-exist in the 122 system and the optimal T_c appears to be achieved at a doping level at which the Neel temperature (T_N) reaches 0K, suggesting the close relationship between the optimal T_c and quantum criticality (electron phase transition at 0K).

The 111- type families

The main representative of the family is LiFeAs which grows in good quality single crystal that cleaved between the two Li layers, thus revealing a non-polar surface with protected topmost FeAs layer. LiFeAs shows superconductivity in the absence of any structural and spin density wave (SDW) transitions [25]. These unique properties prompt further studies on 111 materials to unveil the underlying physics and its relationship with other iron based superconductors. The values of T_c in 11,111 and 122 type iron based superconducting material are shown in table 2.
The 111 type compounds such as AFeAs (A: alkaline elements) with the highest T_c of 18K have the CeFeSi structure (space group P4/nmm). The NaFeAs is another member of the 111 family which shows three successive phase transition at around 52, 41, and 23 K which correspond to structural, magnetic and superconducting transition respectively. Replacing Fe by either Co or Ni suppresses the magnetism and enhances superconductivity. The crystal lattice parameters of LiFeP are smallest among the three 111 compounds (a=3.776 Å & c=6.358 Å).

Table 2 T_c in 111 and 122 type iron based superconductors along with the doping modes and pressure dependence.

System	**Parent compound**	**T_c (K)**	**p *(GPa)***
11 or 111	FeSe	8	-
	FeSe	36.7	8.9
	$FeTe_{0.5}Se_{0.5}$	14	- [26]
	$Fe_{1.01}Se$	36.7	8.9
	$Fe_{1.13}Te_{0.85}Se_{0.1}$	2	-
	$FeTe_{0.8}Se_{0.2}$	10	-
	NaFeAs	33	4
	$NaFe_{0.972}Co_{0.028}As$	31	2.28
	LiFeAs	7	8
	Li_xFeAs	18	
	Na FeAs	9	
122	$CaFe_2As_2$	12	0.5
	$Ca_{0.6}Na_{0.4}Fe_2As_2$	21	-
	$SrFe_2As_2$	40	2.5
	$Sr_{0.6}Na_{0.4}Fe_2As_2$	26	- - [27]
	$BaFe_2As_2$	35	1.5
	$EuFe_2As_2$	41	10
	$Ba_{0.55}K_{0.45}Fe_2As_2$	27	20
	$Ba(Fe_{0.926}Co_{0.074})_2As_2$	10	5.5
	$BaFe(As_{0.65}P_{0.35})_2$	19	38
	$Ba_{0.87}La_{0.13}Fe_2As_2$	30	2.8
	$Ba_{0.6}La_{0.4}Fe_2As_2$	38	-
	$Ba_{0.6}K_{0.4}Fe_2As_2$	38	

The 11 family

This group consists of only Fe and one of the chalcogen elements. The 11-type materials are in iron chalcogenide which started with FeSe having T_c of 8K at ambient pressure [28] and 36.7K with applied pressure of 8.9 GPa. FeSe is formed by alternate stacking of the anti-PbO FeSe layers. FeSe adopts a space group of P4/nmm. This family also includes Fe $Te_{1-x}Se_x$ and $FeTe_{1-x}S_x$. These materials have the simplest structure among iron based superconductors in which iron chalcogenide layer are simply stacked together. The magnetic ground state of FeTe has a double stripe type antiferromagnetic order in which the magnetic moments are aligned antiferromagnetically along the other diagonal direction of the Fe square lattice. The ground state of FeSe has the single-stripe type antiferromagnetic order. For iron Chalcogenides, FeSe has the simplest structure with each unit cell consisting of an FeSe trilayer. Superconductivity above 30K in a FeSe layer compound $K_{0.8}Fe_2Se_2$ achieved by metal K intercalating in between FeSe layers [29]. Each FeSe trilayer corresponds to a selenium-for-arsenic replacement of a FeAs trilayer. The potassium iron selenides [2], K_xFe_{2-y} Se_2 can be viewed as derived from the FeSe system by inserting potassium ions between two FeSe trilayer.
The Fe(Te,Se) bulks prepared by the solid state reaction method always exhibit poor superconducting properties, which are generally believed to be caused by the severe magnetic pair-breaking effect from the inevitable interstitial Fe atoms near the chalcogen planes.

III ELECTRONIC PHASE DIAGRAM

The parent compounds of iron based superconductors exhibit antiferromagnetic ordering at low temperature. It is consensuses that the AF phase deriving from the non-doped parent compound and superconducting phase do not distinctly coexist in the 1111 system, while the two phases do in the 122 system. It is of interest to note that there is a distinct separation between magnetic (PM-AF) and structural (tetra-ortho) transitions in the 1111 system. The undoped parent compound of iron based superconductors show different behaviour. The undoped parent compounds of iron-based superconductors are either superconducting or antiferromagnetic at low temperatures. LaFePO, LiFeAs and FeSe, for example, are nonmagnetic and superconducting even without doping. In contrast undoped LaFeAsO and $BaFe_2As_2$, for example, are non-superconducting antiferromagnetic metals and electron or hole doping suppresses the magnetic order and induces superconductivity. Figure 2 shows the schematic phase diagram of the 1111 and 122 system. The undoped 1111-type iron pnictides show structural and magnetic phase transitions at slightly different temperatures. LaFeAsO undergoes an abrupt structural transition at 155K, changing from high temperature tetragonal structure to low temperature monoclinic structure. At~137K, long range antiferromagnetic order starts to develop. With electron or hole doping, the antiferromagnetic order in the parent compounds is suppressed and superconductivity emerges. For the 1111 system, there is no co-existence between SDW ordering and superconductivity and the T_c appears when the anti-ferromagnetism (AFM) disappears and both of them are connected by a quantum critical point (QCP). On the other hand, the AFM and superconductivity coexist in the 122 system and the optimal T_c appears to be obtained at a doping level where the Neel temperature T_N, the temperature at which an antiferromagnetic material becomes paramagnetic, reached 0 K, suggesting the close relationship between the optimal T_c and quantum criticality.

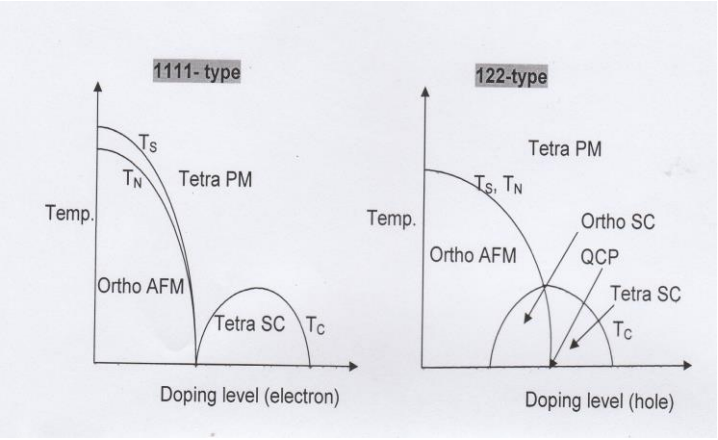

Figure 2 Schematic phase diagrams of the 1111 and 122 system. (T_S= Structural transition temperature, T_N=Neel temperature, SC=superconducting Phase, PM=Pauli Paramagnetism, QCP= Quantum critical Point) .

In $BaFe_2As_2$, the systematic replacement of either the alkaline-earth metal (Ba), transition metal (Fe) or pnictogen (As) with different elements almost universally suppresses the non-conducting antiferromagnetic state of parent compounds to a superconducting non-magnetic state. This phase transition from the antiferromagnetic state to the superconducting state is generic property of the iron based superconductor systems which can also be produced by applied external pressure [30].

IV PAIRING

The electron phonon interaction is not strong enough to give rise to high-T_c in iron based superconductors [31]. It only plays some role in superconducting mechanism by affecting magnetic properties [32]. In iron based superconductivity pairing is a consequence of an unconventional pairing mechanism generated by the electron-electron coulomb interaction. Qualitatively, electrons form pairs under the action of an attractive force that is generated while their mutual coulomb repulsion is avoided. Theoretically, the s±-wave pairing symmetry was proposed for the iron based superconductors [33] Iron based superconductors are multiband systems. There are several bands across the Fermi level. Even if we assume that the pairing has s-wave symmetry, the relative phases of gap functions can be different on different Fermi surface, depending on inter-band pairing amplitudes to be attractive or repulsive. If the gap function has the same phase on all the Fermi surfaces, the pairing is said to have s++ symmetry. On the other hand, if the gap function has opposite phases on different Fermi surfaces, the pairing is said to have s+- symmetry. For iron–based superconductors, if the pairing is induced by AF fluctuations, interaction between Cooper pairs on the electron and the hole bands will generally the repulsive. In this case, the superconducting phases are opposite on the hole and electron Fermi surface, and the gap function has s+- symmetry. However, if the pairing is induced by the orbital fluctuation and the superconducting instability happens, the interaction between Cooper pairs on the electron and hole bands is attractive, and the gap function will have s++ symmetry [34]. Thus, from the relative phases in the gap function, one can determine whether the superconducting pairs are glued by AF fluctuations or by orbital fluctuations. The T_c of iron based superconductors is sensitive to the local geometry of the $FePn(Ch)_4$ tetrahedron. The optimal T_c is achieved when the bond angle of $P_n(Ch)$-Fe-$P_n(Ch)$ approaches that of a regular tetrahedron(109.5^0). The Fermi-surface (FS) dependent nodeless superconducting gaps suggested that inter-FS interactions may play a crucial role in superconducting pairing.

V BAD-METAL BEHAVIOR AND ELECTRON CORRELATION

The metallic phases of iron based superconductors are all characterized by bad metal properties, which provided considerable insight into the degree of electron correlations in these materials. $BaFe_2As_2$ is metallic and develops AFM order at a Neel temperature (T_N) of roughly 140K [35]. Above the T_N it is a paramagnetic metal with a rather large electrical resistivity. They all have a very large electrical resistivity

at room temperature. This property defines a bad metal by the Mott-Ioffe-Regel criterion [36]. The mean free path, l, is very short, of the order of interparticle spacing and its product with the magnitude of the Fermi wave vector,K_F , is of the order of unity. The estimated K_Fl is approximately 5/p ~1 for each Fermi pocket [37]. Because electron phonon scattering gives a much smaller contribution to the resistivity, such a small value of K_Fl in iron pnictides implies strong electron-electron interaction [38].In iron chalcogenides, which are also bad metals with room temperature resistivity reaching Mott-Ioffe-Regel limit, the correlation induced mass enhancement is even larger as large as 20 for some of the involved bands[39]. Electron correlation in iron pnictides and chalcogenides are sufficiently strong to place these materials in the bad metal regime and that frustrated magnetism of local moments describes the dominant part of their magnetic behavior. These bad metal properties suggest that the electron-electron correlations are sufficiently strong to place the metallic iron pnictides and chalcogenides in the proximity of Mott localization. A measure of the strength of the electron correlations is given by the ratio of the local electron-electron interaction to the electron band width or the kinetic energy. Therefore, reducing the kinetic energy would effectively enhance correlation effects. The enhanced electron correlation effects highlight the possibility of observing a Mott insulating state in these materials [40]. The insulating behavior persists above the T_N, a characteristics signature of a Mott insulator. [41]. Insulating behavior has been observed in several other iron chalcogenides. The parent iron pnictides are antiferromagnetically ordered. The AFM order is the background for the quantum fluctuations of the spins below the T_N. The spin fluctuations remain very strong over a wide temperature range above T_N.The electron correlation effects implied by the bad metal behavior have inspired the study of magnetism using local moments as a starting point . Electron correlations turn the majority of the single-electron excitations inherent and distribute them away from the Fermi energy. In many correlated electron materials, there are several competing ground states, and it is often possible to go from one to another through a ‘’quantum Critical point’’ (QCP) by adjusting some control parameter like pressure, magnetic field or chemical composition. Dynamical fluctuations of the order parameter are important for determining the behavior of the system in the neighborhood of the QCP. The quantum critical point (QCP) is the origin of the non-Fermi liquid behavior above T_c. The quantum critical fluctuations help to enhance the superconductivity.

VI APPLICATIONS

Iron based wires and tapes are in the rapid development stage of research and development. The transport J_c= $1.5x10^5$ Acm^{-2} at 4.2 K under 10T was obtained by hot pressing demonstrating their excellent potential for high field applications. The key property of Iron based superconductors relevant for applications is the small anisotropy of J_c with respect to the crystal axis. Further improvement in J_c can be expected upon either introducing more pinning centers or enhancing grain texturing. Superconducting devices based on Josephson junction {42} has been investigated for many years. However, Josephson junctions based phase sensitive devices using iron based superconductors are still facing technological problems. The J_c enhancement in In and Zn added samples may be attributed to the improved phase uniformity as well as the good grain connectivity [42]. Wires and tapes of all Iron based superconductors family[43] have been fabricated by powder in tube (PIT) method and a practical transport J_c ~10^5Acm^{-2} at 10T and 4.2 K has been successfully obtained in $Sr_{0.6}K_{0.4}Fe_2As_2$ tapes [44]. Ex-situ PIT method shows lower impurity phases as well as a high density of the superconducting core for the final wires. Pressure can improve the grain connectivity and increase the pinning number density. Among all iron based superconductors, the 122 type is the most relevant for applications because of its ultrahigh H_{c2} > 70T at 20K [45], low anisotropy (γ<2 for 122) and ease of fabrication. In particular world first 100m-class 122- type Fe based wire was achieved, which demonstrates the great potential for large scale manufacture[46]. Large size bulk iron based superconductor magnets with polycrystalline microstructure would be useful for magnetic levitation, in energy storage application and in compact magnetic resonance devices. The high performance of 30mm diameter iron based superconductor single pancake coil (SPC) in 24T background field clearly demonstrate that iron based superconductors are very promising for high field magnetic applications.

The epitaxially grown $FeSe_{0.5}Te_{0.5}$ thin film with a CeO_2 buffer layer exhibits a superior high field performance with J_c exceeding 10^5Acm^{-2} under magnetic field of 30T at 4.2 K, which is much higher than the conventional superconductor in use [47]. High quality polycrystalline $FeTe_{0.6}Se_{0.4}$ sample prepared by

microwave synthesis method [48] exhibit larger grain size, better grain connectivity, smaller c-axis, high-T_c in magnetic transitions, better M-H loops without magnetic background ,which gives strong indication that there are possibly no interstitial Fe atoms existing in the crystal lattice. The critical current density J_c is greatly enhanced by nearly 30 times to a value about $1.2x10^4 Acm^{-2}$ at 2K and 7T in these polycrystalline bulk materials.

VII COMPARISON OF IRON PNICTIDES WITH MgB_2 AND CUPRATES SUPERCONDUCTORS

Table 3 shows the comparison of three superconductors Iron based superconductors, MgB_2 and Cuprates.

	Iron based superconductors	**MgB_2**	**Cuprates**
Parent material	Antiferromagnetic semimetal (Bad metal) (T_N ~ 150 K)	Pauli paramagnetic metal	Antiferromagnetic Mott insulator (T_N ~ 400 K)
Fermi level	Fe 3d 5-orbitals	B 2p 2-orbitals	Cu 3d single orbitals
Max $T_c(K)$	56 K (for 1111 type) 38K (for 122 type)	40 K	~140K
Correlation effect	Long range(non local) magnetic correlation	None nearly free electron	Strong local electronic interaction
Impurity	Robust	Sensitive	Sensitive
Superconducting gap symmetry	Extended s-wave(+- or ++)	s-wave	d-wave
Upper critical field at 0K,Hc_2 (0)(T)	100–200 T (for 1111 type) 50-100T(for 122 type) ~50 (for 11 type)	~40 T	~100 T
Irreversibility field H_{irr}(T)	>50(4K) >15(20K)	>25(4K) >10(20K)	10(77K,YBCO)
Anisotropy (γ)	2-5	~3.5	4-14
Coherence length(ξ) nm	ξ_c=0.6-1.5 ξ_{ab}=1.5-3	ξ_c=2 ξ_{ab}=10	ξ_c=0.4(YBCO) ξ_{ab}=2.2 (YBCO)
Penetration depth(λ_{ab})nm	~200-500	50	120(YBCO)
Order parameter	One band, sign changing d-wave	Two band, same sign s-wave	One band, sign changing d-wave
Ginzberg number	$1.5x10^{-5}$-$1x10^{-3}$	10^{-5}	$5x10^{-4}$
Pairing interaction	Presumably magnetic	Electron-phonon	Probably magnetic (no consensus)
Crystallographic symmetry in SC state	Tetragonal	Hexagonal	Orthorhombic (Y-and Bi-system
Critical GB angle to keep high J_c	8–9° (Ba 122)	No data	~5° (YBCO)

VII CONCLUSION

The superconducting transition temperature of iron pnictides and chalcogenides are high compared to those of conventional superconductors. The T_c of iron based superconductors is rather low with that of cuprates; the iron based superconductors have distinct advantages in terms of their grain boundary nature, low anisotropy and high crystallographic symmetry of the superconducting phases. The typical Fermi surfaces of iron pnictides comprises hole Fermi pockets in the middle of the Brillouin zone and electron Fermi

pockets at the boundaries. By contrast several iron chalcogenides there are only electron Fermi pockets. Unconventional superconductivity has led to extensive experimental and theoretical studies on the effect of electron correlations and on the nature of magnetism in iron pnictides and Chalcogenides. The PIT wires and tapes and ultrahigh field magnets made of iron based superconductors are cheaper than other superconductors. The investigation of iron-based superconductors may help us to understand the unconventional superconductivity and also provide a new route for searching high-T_c superconductors.

REFERENCES

[1] Fujioka M., et al. 2013. Phase diagram and superconductivity at 58.1K in α-FeAs- free $SmFeAsO_{1-x}F_x$. Supercond. Sci. Technol. 26,085023

[2] Sun L., et al. 2012. Re-emerging superconductivity at 48K in iron Chalcogenides. Nature, 483, 67

[3] Kamihara Y., et al., 2006. Iron based layered superconductor: LaOFeP.J. Am. Chem. Soc. 128, 10012-13

[4] Watanabe T., Yanagi H., et al., 2007. Nickel-based oxyphosphide superconductor with a layered crystal structure, LaNiOP.Inorg. Chem., 46(19) 7719-7721

[5] Kamihara Y., Watanabe T., Hirano M., & Hosono. H., 2008. Iron-based layered superconductor La $[O_{1-x}Fx]$ FeAs (X=0.05-0.12) with T_c=26K. J. Am. Chem. Soc., 130, 3296

[6] Takahashi T., et al., 2008. Superconductivity at 43K in an iron based layered compound $LaO_{1-x}F_xFeAs$. Nature, 453,376

[7] Ren Z.A., Lu W.,Yang J., et al. 2008. Superconductivity at 55K in iron based F-doped layered quaternary compound $SmO1_{-x}F_xFeAs$. Chin. Phys. Lett., 25, 2215

[8] Wang C., Li L., Chi S., et al. 2008. Thorium –doping induced superconductivity up to 56K in $Gd_{1-x}Th_xFeAsO$. Europhys. Lett. 83, 67006

[9] Wu G., et al., 2009. Superconductivity at 56K in samarium doped SrFeAsF. J. Phys. Cond. Matter.21, 142203

[10] Cheng P., et.al., 2009. High T_c Superconductivity induced doping rare earth elements into CaFeAsF. Europhys. Lett. 85, 67003,

[11] Ogino H., Matsumura Y., et.al. 2009 .Superconductivity at 17K in $(Fe_2P_2)(Sr_4Sc_2O_6)$: a new superconducting layered Pnictide oxide with a thick perovskite oxide layer. Supercond. Sci. technol. 22, 075008

[12] Ma F.J., Lu Z.Y, Xiang T., 2008. Arsenic bridged antiferomagnetic super exchange interactions in LaFeAsO. Phys. Rev. B, 78,033111

[13] Singh D.J., 2009. Electronic structure of Fe based superconductors. Physica C, 469,418

[14] Chen F., et al., 2010. Electronic structure of $Fe_{1.04}Te_{0.66}Se_{0.34}$. Phys. Rev. B., 81, 014526

[15] Takahashi H., et al., 2008. Superconductivity at 43K in an iron based layered compound $LaO_{1-x}F_xFeAs$. Nature (London) 453,376-378

[16] Lu X.F., Wang N.Z., et al. Superconductivity in $LiFeO_2Fe_2Se_2$ with anti-PbO-type spacer layers. Phys. Rev. B., 2013, 89, 020507(R)

[17] Chen G.I.,et al, 2008.Superconductivity at 41K and its competition with spin density wave instability in layered $CeO_{1-x}F_xFeAs$., Phys. Rev. Lett. 100, 247002

[18] Ren Z.A., et al., 2008. Superconductivity at 52 K in iron based F doped layered quaternary compound $[O_{1-x}F_x]$ FeAs. Mater. Res. Innov. 12,105-106

[19] Tarashima, K., et al., 2009. Fermi surface nesting induced strong pairing in iron-based superconductors. Proc. Natl. Acad. Sci., 106, 18, 7330

[20] Hasimoto K., et al., 2012. Isotopic superconducting gaps with enhanced pairing on electron Fermi surfaces in $FeTe_{0.55}Se_{0.45}$. Phys. Rev. Lett., 108,047003

[21] Yi M., et al., 2009. Electronic structure of $BaFe_2As_2$ family of iron-pnictide superconductors. Phys. Rev. B, 80, 024515

[22] Miao H., et al. 2015. Observation of strong electron pairing on bands without Fermi surface in $LiFe_{1-x}Co_xAs$. Nature. Comm. 6, 6056

[23] Johnston D.C., 2010. The puzzle of high temperature superconductivity in layered iron pnictides and chalcogenides. Adv. Phys., 59, 6, 1063

[24] Lv B., Deng L .Z. and Gooch M., et al., 2011. Unusual superconducting state at 49K in electron doped $CaFe_2As_2$ at ambient pressure.Proc. Natl. Acad. Sci. (USA), 108, 15705-9,
[25] Tapp J.J., Tang Z., Lv .B., et al., 2008. LiFeAs: An intrinsic FeAs-based superconductor with T_c =18K. Phys. Rev. B, 78, 060505(R)
[26] Sales. B.C. et al., 2009. Bulk superconductivity at 14 K in single crystal of $Fe_{1+y}Te_xSe_{1-x}$. Phys. Rev. B, 79, 094521
[27] Cortes Gill R., and Clarke S.J., 2011. Structure, magnetism, and superconductivity of the layered iron arsenide's $Sr_{1-x}Na_xFe_2As_2$., Chem. Mater. 23, 1009-1016
[28] Hsu F.C., LuO J.Y., and Yeh K.W., et al., 2008. Superconductivity in the PbO type structure α-FeSe. Proc. Natl, Acad. Sci. U.S.A. 105, 14262-264
[29] Guo J., 2010. Superconductivity in the iron selenide $K_xFe_2Se_2(0\leq x\leq 1.0)$ Phys. Rev. B, 82, 180520
[30] Park T., et al., 2008. Pressure-induced superconductivity in $CaFe_2As_2$. J. Phys. Condens. Matter, 20(32), 2204
[31] Boeri L., et al., 2008. Is $LaFeAsO_{1-x}F_x$ an electron –phonon superconductor? Phys. Rev. Lett. 101, 026403
[32] Bang Y., 2009. Isotopic effect and the role of phonons in the iron based superconductors. Phys. Rev. B, 79, 092503
[33] Kuroki K., et al., 2008. Unconventional pairing originating from the disconnected Fermi surfaces of superconducting $LaFeAsO_{1-x}F_x$. Phys. Rev. Lett, 101, 087004
[34] Onari S and Kontani H., 2009. Violation of Anderson's theorem for the sign Reversing s-wave state of iron Pnictide superconductors. Phys. Rev. Lett., 103,177001
[35] Dai P., 2015. Antiferromagnetic order and spin dynamics in iron-based superconductors. Rev. Mod. Phys. 87,855
[36] Hussy N.E., et al., 2004. Universality of the Mott-Ioffe-Regel limit in metals. Philos. Mag. 84(27), 2847
[37] Abraham E., et al., 2011., J. Phys. Condens. Matter, 23, 223201
[38] Qazilbash. M. M., J.J. Hamlin., et al, 2009. Electronic correlations in the iron Pnictides. Nature. Phys., 5, 647
[39] Yi. M., Liu Z.K., et al., 2015. Observation of universal strong orbital-dependent correlation effects in iron Chalcogenides. Nature Commun. 6, 7777
[40] Zhu J .X., et al., 2010. Band narrowing and Mott localization in iron oxychalcogenides $La_2O_2Fe_2O(Se,S)_2$, Phys. Rev. let. 104,216405
[41] Imada. M., Fujimon & Tokura.Y., 1998. Metal Insulator transitions. Rev. Mod. Phys.70, 1039
[42] Shrivastava Shailaj Kumar and Girijesh Kumar., 2019. Application of high-T_c superconducting Josephson devices. International Journal of Emerging Technologies and innovative Research (JETIR), 6(1) 517-523
[43] Hosono H., et al., 2018. Recent advances in iron based superconductors towards applications. Mater. Today.21 (3), 278-302
[44] Pyon S., et al. 2018.Improvement of fabrication processes and enhancement of critical current densities in $(Ba,K)Fe_2As_2$ HIP wires and tapes . Supercond. Sci. Technol. 31(5), 055016
[45] Gurwich A., 2011. To use or not to use cool superconductors? Nat. Mater10 (4), 255-259
[46] Zhang X et al., 2014. Realization of practical level current densities in $Sr_{0.6}K_{0.4}Fe_2As_2$ tape conductors for high field applications .Appl. Phys. Lett. 104,202601
[47] Yuan P.S. et al 2015. High performance FeSe0.5Te0.5 thin films grown at low temperature by pulsed laser deposition. Supercond. Sci. Tecnol. 28(6), 065009
[48] Pan B.J., Zhao K., Liu. T., Ruan B.B. and Zhang S. et al. 2019. Direct microwave synthesis of 11-type Fe(Te,Se) polycrystalline superconductors with enhanced critical current density. Chin. Phys. Lett. 36,017401